Vibrational mode-specific photochemical reaction dynamics of chlorine dioxide in solution

Henk Fidder, Frank Tschirschwitz, Oliver Dühr, and Erik T. J. Nibbering

Citation: The Journal of Chemical Physics **114**, 6781 (2001); doi: 10.1063/1.1357202
View online: http://dx.doi.org/10.1063/1.1357202
View Table of Contents: http://scitation.aip.org/content/aip/journal/jcp/114/15?ver=pdfcov
Published by the AIP Publishing

Vibrational mode-specific photochemical reaction dynamics of chlorine dioxide in solution

Henk Fidder[a)]
Department of Physical Chemistry, Uppsala Universitet, P.O. Box 532, S-751 21 Uppsala, Sweden

Frank Tschirschwitz, Oliver Dühr, and Erik T. J. Nibbering
Max-Born-Institut für Nichtlineare Optik und Kurzzeitspektroskopie, Max Born Strasse 2A, D-12489, Berlin, Germany

(Received 25 April 2000; accepted 29 January 2001)

We study the reaction dynamics of OClO in cyclohexane, acetonitrile, and water by femtosecond pump–probe spectroscopy. In all solvents we observe a quantum beat in a 403 nm one-color pump–probe experiment with 55 fs temporal resolution, that decays with a 1.3–1.5 ps time constant. From this we conclude that, in contrast to previous reports, not all OClO molecules dissociate after excitation with 403 nm light. In both cyclohexane and water we observe in the 403 nm experiment an increase in stimulated emission between 0.5 and 2 ps that appears to be connected to the quantum beat decay. We explain these results as the consequence of vibrational relaxation of the bending mode of OClO. Relaxation from $(\nu_1,1,0)$ to $(\nu_1,0,0)$ leads to population of a state with a two times higher transition dipole moment, which accounts for the increased stimulated emission. Further proof that not all OClO molecules dissociate immediately after excitation is found in the identification of a stimulated emission contribution in femtosecond 400 nm pump/800 nm probe experiments, which also decays with about a 1.5 ps time constant. Femtosecond 400 nm pump/267 nm probe measurements indicate that a fraction of the OClO molecules dissociate very rapidly, with dissociation times of $\leqslant$60, 80, and 140 fs, in acetonitrile, water, and cyclohexane, respectively. An anisotropy decay is resolved at 267 nm of the formed ClO in water and cyclohexane, with anisotropy decay times of 0.17 and 0.27 ps, respectively. In all solvents a fraction of the ClO+O fragments recombine, with time constants of 1.2 and 4.1 ps in water, 6.0 ps in acetonitrile, and 8.9 ps in cyclohexane. In acetonitrile a secondary dissociation pathway is identified with a 2.1 ps time constant. This pathway might also be responsible for the biexponentiality of the recombination process in water. In particular, in acetonitrile and cyclohexane the data indicate cage escape of a significant amount of fragments. © *2001 American Institute of Physics.*
[DOI: 10.1063/1.1357202]

I. INTRODUCTION

The object of our studies is the ultrafast photo-induced reaction dynamics of the three-atomic molecule OClO in liquid solution (see Fig. 1). This molecule has met with considerable interest over the last two decades, particularly due to the possible involvement of OClO and its photochemical products in the ozone depletion of the atmosphere.[1] An aspect that makes the OClO molecule very interesting for studies of reaction mechanisms is that it has been found to break up in two ways, either giving ClO+O, or Cl+O_2.[1,2] Thus, in a molecule with only three atoms a competition exists between at least two exit channels. In contrast, only one reaction channel exists in the studies of ICN,[3] NaI,[4] I_2,[5–10] IBr,[11] CH_3I,[12] I_2^-,[13,14] BrI_2^-,[15] or two indistinguishable channels in the case of I_3^-,[16–20] HgI_2,[21,22] $HgBr_2$,[22] and CH_2I_2.[23,24] On top of this OClO can also undergo isomerization to ClOO.[25] In low temperature solid matrix (argon,[26–29] neon,[27,28] krypton,[28] amorphous,[29] and polycrystalline[30] ice) studies ClOO proved to be the dominant end product, possibly formed after recombination of ClO+O. A further point of importance is that OClO has only three vibrational degrees of freedom. As a consequence the density of molecular levels is relatively sparse, which strongly reduces the number of intramolecular vibrational energy redistribution (IVR) pathways.[31] Therefore, reaction dynamics characteristics of individual vibronic levels might be identified in OClO. This in contrast to typical dye molecules containing a few dozens of atoms, where IVR and energy exchange with the solvent typically lead to a rapid relaxation to the vibrationally unexcited electronic state.

Electronic excitation of OClO occurs from the $X\,^2B_1$ ground state to the optically accessible $A\,^2A_2$ state (Fig. 2).[32] The complexity of OClO photodissociation is partially due to two other, optically inaccessible, electronic excited states with about the same internal energy as the $A\,^2A_2$ state. Strong interactions between these three excited electronic states are thus expected to occur. Peterson and Werner have shown that the $A\,^2A_2$ state interacts through spin–orbit coupling with the $1\,^2A_1$ state.[32–34] Vibronic coupling exists between the $1\,^2A_1$ and $1\,^2B_2$ states. The magnitude of the coupling between these states can be expected to be modulated

a)Electronic mail: henk.fidder@fki.uu.se

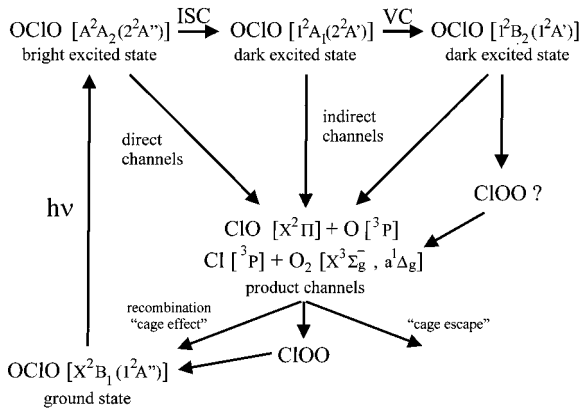

FIG. 1. Flow scheme of the possible photochemical reaction pathways of OClO as previously known from the literature. The electronic state indices $X\,^2B_1$, $A\,^2A_2$, $1\,^2A_1$, and $1\,^2B_2$ transform under symmetry operations in the symmetry point group C_{2v}; the indices $1\,^2A''$, $2\,^2A''$, $2\,^2A'$, and $1\,^2A'$ are the corresponding indices in the case of the point group C_s. We note that the asymmetric dissociation channel OClO→ClO+O should be described in the C_s group. For details see the text.

by the surrounding solvent. Studying the cuts through the potential energy surfaces (PESs) along different vibrational coordinates calculated by Peterson and Werner[32] (reproduced in Fig. 2), we can get some idea of what might happen after excitation to the $A\,^2A_2$ PES. Along the symmetric stretch vibrational coordinate (ν_1) the molecule cannot dissociate, but relaxation might occur to the dark states $1\,^2A_1$ and $1\,^2B_2$, which both are not dissociative along the symmetric stretch coordinate ν_1. Along the bending coordinate (ν_2) the molecule is bound on the $A\,^2A_2$ surface, which is crossed by the $1\,^2A_1$ surface near the bottom. Relaxation to the $1\,^2A_1$ surface is a potential pathway for dissociation since this surface appears to have only a small barrier towards dissociation. Along the asymmetric stretch coordinate (ν_3) dissociation can occur on all three PESs, the difference being that on both the $A\,^2A_2$ and the $1\,^2A_1$PES there is a barrier to cross, whereas the $1\,^2B_2$ PES does not have a barrier towards dissociation.

The absorption spectrum of the OClO molecule is dominated by progressions of vibronic lines (ν_1,ν_2,ν_3) in the Franck–Condon active symmetric stretch (ν_1) mode,[35,36] associated with the $X\,^2B_1 \rightarrow A\,^2A_2$ electronic transition (see Fig. 3). Vibronic states (ν_1,0,0), where only ν_1 is excited, have the strongest transition moments.[36] Combination bands where the symmetric stretch is excited, together with the bending mode, the asymmetric stretch mode, or both, are also observed. These lead to additional progressions of the type (ν_1,1,0), (ν_1,0,2), (ν_1,1,2), and (ν_1,0,4).

Extensive experimental work on OClO in the gas phase has been performed.[37–49] Richard and Vaida[39] found that vibronic states with excitation of the ν_2 bending mode or ν_3 asymmetric stretch mode have larger linewidths than states with only excitation of the ν_1 symmetric stretch mode, which suggests that these modes might expedite the predissociation process. Bishenden and Donaldson[40,41] found that the ClO $X(\nu=4)$ product yield (excitation 356 to 370 nm) is 2–3 times higher if the asymmetric stretching mode is excited, than for the other vibronic transitions. Davis and Lee[42] concluded that the $Cl+O_2$ channel reaches a maximum yield of 4% for 404 nm excitation. Below 400 nm (>3.1 eV) the yield of this channel sharply decreased, indicating that a new dissociation channel to ClO+O becomes available. Furthermore, they concluded that the yield of the $Cl+O_2$ channel is about ten times lower when additional energy is deposited in the asymmetric stretching mode.[43] Both results indicate that the ν_3 asymmetric stretching mode promotes the ClO+O photodissociation channel. Energy partitioning into transla-

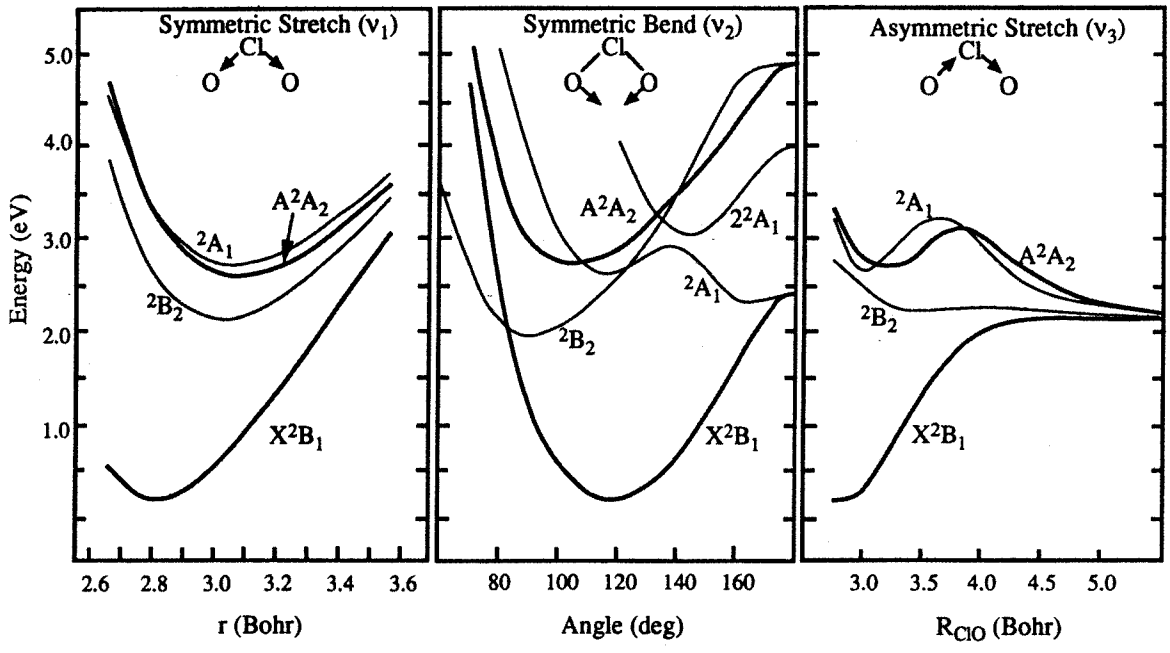

FIG. 2. Cuts through the *ab initio* potential energy surfaces as calculated by Peterson and Werner (taken from Ref. 32).

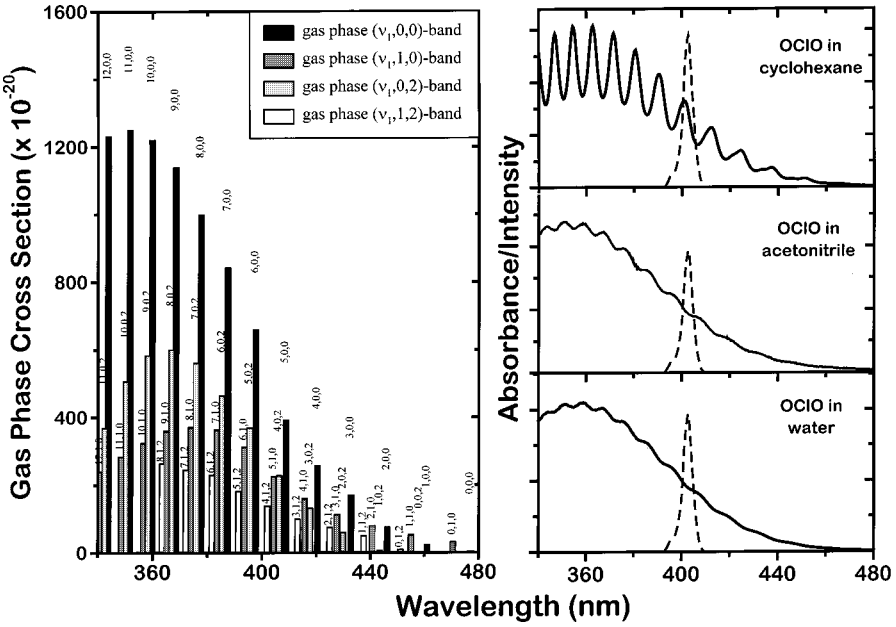

FIG. 3. Absorption spectra of OClO in cyclohexane, acetonitrile, and water, together with the gas phase stick spectrum constructed from the results of Hubinger and Nee (Ref. 36). The spectrum of the pump pulse around 400 nm is depicted as the dashed line.

tional, vibrational, and rotational degrees of freedom of the photodissociation products has been determined.[42–47] From these cw gas phase studies the picture has emerged that the lifetimes of the excited state and outcome of the photochemical reactions depend on the vibronic mode that has been excited.

Ultrafast time-resolved gas phase studies of OClO by Baumert *et al.*[48] with pumping between 308–352 nm demonstrated biexponential wavelength-dependent dissociation dynamics, suggesting the existence of at least two dissociation channels. The two lifetimes varied in the range of ~30 to ~500 fs. Ludowise *et al.*[49] produced a quantum beat signal from a superposition of the (7,0,0) and the (6,0,2) vibronic states. They found a 4.2 ps and 2.0 ps lifetime for the (7,0,0) and the (6,0,2) state, respectively. From a 250 fs delay for the rise of the ClO signal they concluded that the 4.6 ps relaxation is to an intermediate state with a 250 fs lifetime ($1\,^2A_1$ and/or $1\,^2B_2$ states), from where dissociation to ClO+O takes place.

Several studies of ultrafast reaction dynamics of OClO in solution have been reported. Most work has been on OClO in water. Simon and co-workers[50–53] performed the first time-dependent studies of OClO reaction dynamics in solutions. Their first studies[50–52] had ~80 ps time resolution, which is too low to capture the fast reaction dynamics. These data mainly reflect the absorption changes due to the solvent-dependent mixture of end products Cl, ClO, O, and ClOO.[50–52] They concluded that in water 90% of the OClO molecules dissociates to ClO+O, and only 10% to $Cl+O_2$.[52] In a later study with femtosecond time resolution on OClO in water,[53] with excitation at 395 nm, they observed transients between 400 and 700 nm that they assigned to vibrational energy relaxation (VER) of vibrationally hot ClOO, which they claim is formed within 0.7 ps.

Keiding and co-workers[54–56] concluded from studies with femtosecond time resolution on OClO in water that there are no strong indications for formation of ClOO. They demonstrated that in water OClO mainly dissociates to ClO+O and conclude that almost all these fragments recombine within 0.8 ps to form OClO again,[54] vibrationally hot and on the ground state PES.[56] Signals between 459 and 1024 nm, after excitation at 400 nm, were described by VER on the OClO ground state PES.[56] The original bleach was found to recover almost entirely, leaving a quantum yield of only about 7% for the $Cl+O_2$ dissociation channel,[54] a yield similar to what Dunn *et al.*[52] had previously concluded. They also showed that the signal spectrum after 40 ps corresponds very well to the absorption spectrum of Cl radicals in water, which indicated that in water Cl and O_2 are the only surviving end products.[54] A recent time-resolved resonance Raman study by Thomsen *et al.*[57] provided direct evidence for the formation of ClOO after excitation of OClO in water, based on the appearance of a vibrational band at 1442 cm^{-1}, which corresponds to one of the vibrational frequencies of ClOO. This band was found to appear 12.7 ps delayed and with a rise time of 27.9 ps, and the signal decayed with a time constant of 398 ps.

Apart from Dunn *et al.*,[52] only Reid and co-workers[58–64] have published data on OClO in solvents other than water. In a time-resolved subpicosecond study on OClO in water and acetonitrile,[58,59] they found that their data in water supported the interpretation of Keiding and co-workers.[54–56] However, in acetonitrile they assigned the signals for probing at 800 nm after excitation at 400 nm to vibrationally hot ClOO,[58,59] in line with the previous interpretation by Chang and Simon[53] for OClO in water. Reid and co-workers also published a number of papers on resonance Raman investigations of the OClO reaction dynamics in cyclohexane,[60,61] acetonitrile,[62] and water.[62–64] Their main conclusions[60,61,63] are that the PES for the asymmetric stretch coordinate is dramatically altered in solution compared to the gas phase, and that depolarization of the symmetric stretch Raman line indicates influence of the $X\,^2B_1 \rightarrow 1\,^2A_1$ transition that has

not been observed in any absorption experiment so far. In time-resolved resonance Raman measurements, Reid and coworkers have found that in the geminate recombination of ClO+O and the subsequent vibrational relaxation in the $X\,^2B_1$ state the excess vibrational energy is deposited along the asymmetric stretch coordinate.[62,64]

Summarizing, we mention that the bulk of work on OClO in solution has been done for the solvent water. A coherent interpretation for the reaction dynamics in this solvent has emerged. Nevertheless, due to our higher time resolution and the larger spectral bandwidth of our laser pulses we have observed and time-resolved new features, which compel us to introduce some important modifications to the prevailing interpretation. Our data on the solvents acetonitrile and cyclohexane provide additional information on OClO reaction dynamics that we could not have determined from the water data alone. Combined, these data lead to a more complex picture of reaction dynamics of OClO in solvents than exists so far. From our measurements we conclude that the photodissociation dynamics of OClO in liquid solution is dependent on which vibronic level is excited within the $A\,^2A_2$ state.

II. EXPERIMENT

Pump–probe measurements were performed on a home-built 1-kHz amplified Ti:sapphire laser system, which has been described elsewhere.[65,66] Frequency conversion of the laser output of 1.2 mJ 40 fs pulses centered at 800 nm in 100 μm BBO cut at 27° resulted in 200 μJ 40 fs pulses at the second harmonic frequency. These were used in the single-color pump–probe experiments where the pulses were centered at 403 nm. In the two-color experiments half of the fundamental energy was used for frequency conversion to give 100 μJ of the second harmonic; the other half was used either as a probe or as a mixing beam for third harmonic generation. Half of the energy of the second harmonic was used as the pump beam for both the 400/800 and the 400/267 nm experiments. In the 400/267 nm pump–probe experiments the other half of the second harmonic beam was upconverted to the third harmonic with the remainder of the fundamental beam in a 100 μm BBO crystal cut at 45°. Cross correlation between the 400 and 800 nm beams in a 100 μm thick BBO crystal resulted in correlation widths of 70–75 fs, from which we conclude that the pulse widths are 50–60 fs. In gas phase experiments the cross-correlation width between the 400 and 267 nm beams was 65–70 fs. This leads us to conclude that the third harmonic also had a pulse width of 50–60 fs. Polarization rotators and Glan–Taylor prisms were inserted in the probe beams to study anisotropy effects. The inclusion of these additional optical elements in the pump and probe beams resulted in only minor pulse lengthening effects. In these anisotropy measurements the probe polarization was rotated to 45°, with respect to the pump polarization. Probe transmission through the sample was then measured simultaneously for both the parallel and perpendicular components (400/800 nm experiments) or directly after each other (400/267 nm experiments).

In all cases the pump–probe signal was measured after optically pumping the $X\,^2B_1 \rightarrow A\,^2A_2$ transition at 400 nm. The pump–probe experiments were performed at room temperature on 500 μm thick flow cells with 1 mm thick CaF_2 windows. Fused silica or BaF_2 windows turned out to have lower damage thresholds than CaF_2 when exposed to chlorine dioxide and the radicals formed after photoexcitation. The relative large sample thickness was necessary to obtain a sufficiently good signal-to-noise ratio. Group velocity mismatch (GVM) between 400 and 800 nm, and between 400 and 267 nm, decreased the temporal resolution to about 160–250 fs, as indicated by the width of the multiphoton processes signal at zero delay. These multiphoton peaks were also detected in the pure solvent. However, a possible contribution of the cell windows to the multiphoton peaks should not be discarded, in particular for the 400 nm/267 nm experiments, and the stated values should be considered as an upper limit. The relevant signals, on the other hand, will only experience GVM from OClO and the solvent. Therefore, we estimate that the effective temporal resolution is more likely to be on the order of 120–150 fs in the two-color experiments. However, in our analysis of the two-color experiments we will use the upper limit values characterized by the multiphoton peaks.

The laser beams were focused with an aluminum mirror with $R = 30$ cm radius of curvature. Pump intensities were less than 10 GW/cm^2 at the focus, well below the threshold of self-phase modulation. Measurements were performed with lower pump intensities to check the linearity of the response to pulse energy density.

Solutions of OClO in cyclohexane, acetonitrile (both Merck, analytical grade), and doubly deionized water were prepared using the method of Bray.[67] Oxalic acid (Merck) and potassium chlorate (Aldrich) were mixed with a few drops of water and heated to 60 °C. The resulting gaseous mixture of OClO and CO_2 was bubbled through the used solvents. The resulting solutions were used as obtained. Typical optical densities at 400 nm were 0.5–0.6 for the 500 μm thick samples.

Measurements of electronic absorption spectra were performed before, during, and after the pump–probe experiments to check for possible degradation of the used solutions.

III. RESULTS AND DISCUSSION

This section is structured as follows. In Sec. III A we describe what contributions might be expected at the various probe wavelengths following pumping at 400 nm. In Sec. III B we discuss the origin of the quantum beat feature that the 403 nm pump/403 nm probe traces have in common for all solvents. In Sec. III C we present a flow scheme of the OClO reaction dynamics we obtain from our experiments, and give particulars concerning the fit functions that we used to describe our data. In Secs. III D–III F we describe our data and present our interpretation of the reaction dynamics of OClO in cyclohexane, acetonitrile, and water, respectively. In Sec. III G we compare the results for the different solvents and draw some general conclusions.

A. Possible pump–probe signal contributions

In Fig. 3 parts of the electronic absorption spectra of OClO in cyclohexane, acetonitrile, and water are given, together with a stick spectrum representing the gas phase data by Hubinger and Nee.[36] We have performed some preliminary fits on the absorption spectra that indicate that the cyclohexane, acetonitrile, and water spectra are redshifted compared to the gas phase spectrum by about 275, 0, and 150 cm^{-1}, respectively. In these fits we broadened the gas phase spectrum by convoluting the stick spectrum with a Gaussian. The full width at half maximum (FWHM) of the Gaussian required in the convolutions is 435, 680, and 705 cm^{-1}, for cyclohexane, acetonitrile and water, respectively. Keiding and co-workers[56] modeled the OClO absorption spectrum in water using a FWHM of 525 cm^{-1}. For cyclohexane, which has the most structured absorption spectrum, these preliminary fitting results suggest that the relative strength of the different transitions differs somewhat in cyclohexane from the gas phase. In addition, in the onset range of the cyclohexane absorption spectrum some of the simulated peaks fall in between the experimental peaks, while the main progression, which is only related to the ν_1 symmetric stretch vibrational frequency, is accurately reproduced. This indicates that the frequency of the symmetric stretch mode has not changed noticeably in cyclohexane compared to the gas phase; however, it suggests that the other modes might have altered frequencies! Notice that since there are no actual progressions in the other modes, a difference is most likely to be discerned in the onset range of the absorption spectrum. A comparison of the absorption spectra in water of OClO and the products Cl and ClO, as well as the gas phase spectrum of the possible intermediate ClOO, can be found in Ref. 56.

1. Pump 400 nm—probe 267 nm

This experiment allows for most options of contributing entities. Near 267 nm the ClO radical has its absorption maximum.[68] The Cl radical, that peaks near 310 nm in H_2O, still has about a three times higher extinction coefficient at 267 nm than the ClO radical.[68,56] The ClOO molecule has an absorption maximum at 247 nm in a neon matrix,[27] but its extinction coefficient is still comparable to that of ClO at 267 nm. Only OClO itself has a negligible absorption at 267 nm.[55]

2. Pump 403 nm—probe 403 nm

There seems to be good agreement between most authors[53–56,58,59] that signals at 403 nm after pumping around 403 nm are mainly related to ground state bleaching and stimulated emission from the excited $A\,^2A_2$ state. The data around 400 nm for OClO in water usually show a small residual contribution which is related to the $Cl+O_2$ channel. Below 390 nm the Cl–water charge transfer complex absorption exceeds this tiny contribution resulting in a net increased absorption.[55] By inspection of Figs. 4–7 it is clear that in all solvents a quantum beat signal persists up to several picoseconds. This indicates that a significant fraction of the OClO molecules does not dissociate on a time scale of less than 1 ps.[53–56,58,59]

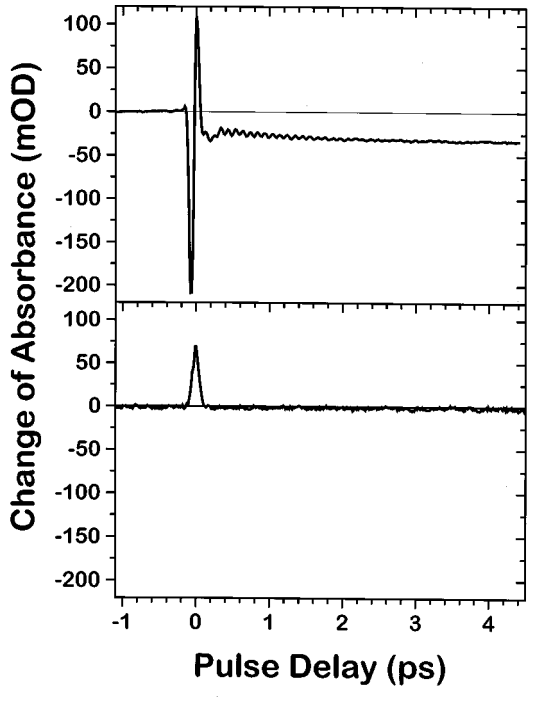

FIG. 4. The 403 nm/403 nm pump probe data on OClO in cyclohexane (upper panel). The lower panel shows the signal from pure cyclohexane.

3. Pump 400 nm—probe 800 nm

The signal at 800 nm after pumping at 400 nm is composed of two contributions: a stimulated emission and an increased absorption contribution (see Figs. 5–7). For OClO in water the increased absorption signal at 800 nm has been assigned by Keiding and co-workers[56] to absorption from vibronically hot OClO on the ground state PES. They convincingly demonstrated, by modeling the decay dynamics data over the range of 400 to 1200 nm, that these signals are related to vibrational relaxation on the $X\,^2B_1$ ground state PES of OClO. The almost complete recovery of the bleach at 400 nm in water after 20 ps also indicates that most OClO molecules are restored to their original state.[58] The stimulated emission contribution has not previously been ascribed to the OClO molecule.[58,59] We assign this contribution to stimulated emission from OClO molecules in the $A\,^2A_2$ excited state to high vibrational levels on the ground state PES, basically the reverse of the increased absorption transition.

B. Origin of the quantum beat

All 403 nm pump/403 nm probe signals show a quantum beat during the first few picoseconds, with an identical beat frequency of 101 fs ($\sim$330 cm^{-1}) and a decay constant for the amplitude of 1.3–1.5 ps (see Figs. 4–7). In Fig. 4 we illustrate for OClO in cyclohexane that this signal is not related to the solvent. The existence of this quantum beat implies that, in contrast to what has been said in the literature for OClO in water, not all OClO molecules dissociate and recombine within 0.7–0.8 ps.[53,54] Since initially there are only OClO molecules absorbing at this wavelength they have to be responsible for the coherence. The quantum beat fre-

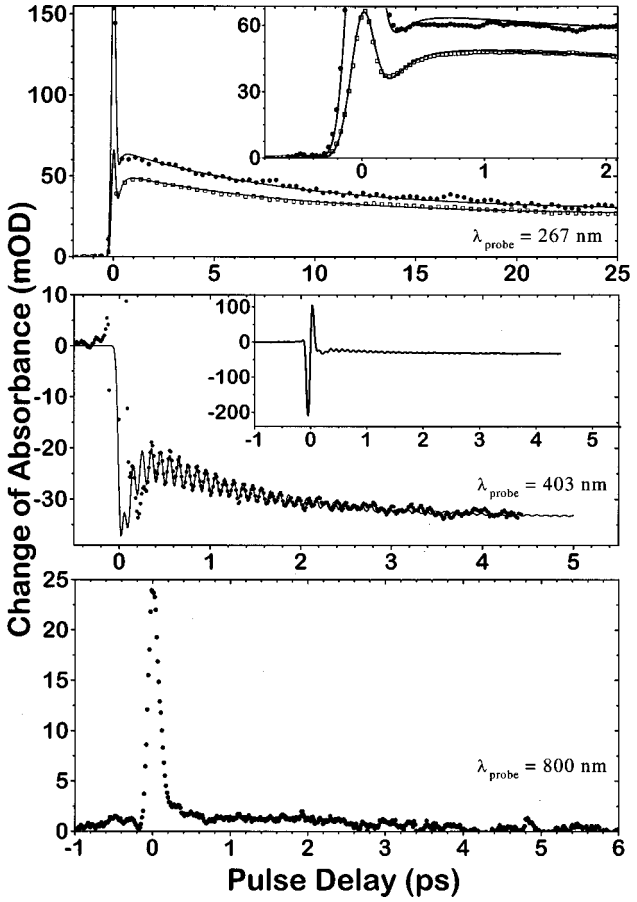

FIG. 5. Data and fits for the transient pump–probe data obtained on OClO in cyclohexane. The upper panel contains the 267 nm data for OClO in cyclohexane, fitted according to Eqs. (6) and (7) (solid lines). The solid dots are the data for parallel polarization; the open squares are the data for perpendicular polarization. These data have not been scaled to each other. The spike around zero delay is due to a multiphoton absorption process. The inset shows the rise due to ClO formation and anisotropy decay in greater detail. The middle panel shows the 403 nm fit on OClO in cyclohexane using Eq. (8), together with the experimental data (dots). The inset shows the strong coherent coupling between pump and probe in the data around zero delay. The lower panel shows the strong coherent signal observed at 800 nm.

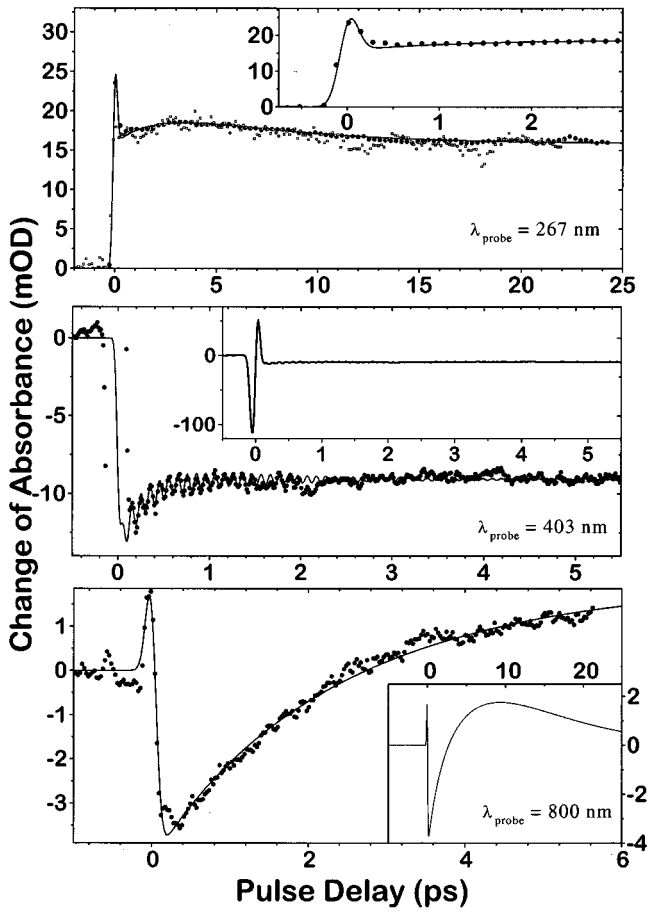

FIG. 6. Data and fits for the transient pump–probe data obtained on OClO in acetonitrile. The upper panel shows the fit (solid line) according to Eq. (9) to our 267 nm data (solid dots) obtained on OClO in acetonitrile for parallel pump and probe polarization. The open squares are the data for perpendicular pump probe polarization. The spike around zero delay is due to a multiphoton absorption process. The middle panel shows the fit curve to our 403 nm data using Eq. (10) (solid line) together with the experimental curve (dots). The inset shows the strong coherent coupling between pump and probe in the data around zero delay. The lower panel shows the fit to our 800 nm data obtained on OClO in acetonitrile using Eq. (11) (solid line) together with the experimental data (dots). The spike around zero delay is due to a multiphoton absorption process. The inset shows the longer time behavior of the transient as predicted by Eq. 11 (compare to Ref. 58).

quency poses some difficulty, since it does not connect to any vibrational frequency or accessible combination of vibronic transitions as known from the gas phase absorption spectra.[35,36] In addition, a contribution from a ground state wave packet created by a stimulated Raman excitation process is also unlikely, since the lowest vibrational frequency in the $X\,^2B_1$ ground state is 448 cm^{-1}. Furthermore, we mention that the $X\,^2B_1$ ground state vibrational frequencies are considerably larger than kT; therefore, OClO is mainly excited from the (0,0,0) vibrational mode.

It is possible that, going from the gas phase to the solvent phase, vibrational frequencies and energy separations are altered. We find indications for this in the electronic absorption spectra (see Sec. III A) and the emission spectra analysis of OClO in solid neon, argon, and krypton matrices at low temperatures by Liu *et al.*[31] Nearly all modes appear to have slightly higher vibrational frequencies in noble gas matrices than in the gas phase, both in the $X\,^2B_1$ state and the $A\,^2A_2$ state. In all cases the change in frequency is about 1% or less, except for the excited state bending mode, where increases by as much as 5% to 303.0 cm^{-1} in Kr matrices occur, compared to 288.1 cm^{-1} in the gas phase. This clearly opens the possibility for a further increase in vibrational frequency of OClO dissolved in molecular liquids. We are faced with the consequence that the vibrational frequency not only has to deviate substantially from those derived for the gas phase, but also this deviation has to be identical in all the solvents we used. We propose that the bending mode (ν_2) is the best suitable candidate, since it exhibits the largest change in frequency in noble gas matrices, and because it is the only mode that has a lower frequency in the gas phase ($\sim$288 cm^{-1}) than the observed 330 cm^{-1} for the quantum beat. The increase in frequency can be visualized as the result of a steepening of the PES of this vibration caused by a lack of free space in the solvent to perform the vibrational motion. This would explain why the increase is similar for

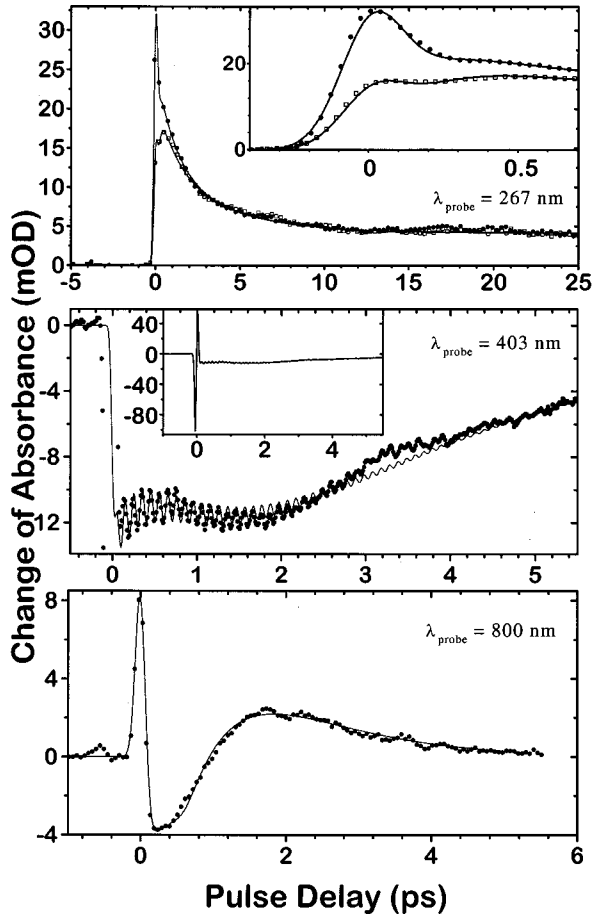

FIG. 7. Data and fits for the transient pump–probe data obtained on OClO in water. The upper panel shows the fits of our 267 nm data obtained on OClO in water according to Eqs. (12) and (13) (solid lines). The solid dots are the experimental data for parallel polarization; the open squares are the experimental data for perpendicular polarization. The spike around zero delay is due to a multiphoton absorption process. The inset shows the rise due to ClO formation and anisotropy decay in greater detail. The middle panel shows our 403 nm data on OClO in water (dots) and the fit described by Eq. (14) (solid line). Again, the inset shows the strong coherent coupling signal in the data around zero delay. The lower panel shows our 800 nm data (dots) obtained on OClO in water, together with the fit given by Eq. (15) (solid line). The spike around zero delay is due to a multiphoton absorption process.

the different solvents, since the amount of unoccupied space does not vary dramatically from solvent to solvent.

The quantum beat reflects the interference of the polarizations on two different vibronic transitions. Based on gas phase work[40–43] and data presented in Secs. III D–III F we propose that states of the type $(\nu_1,\nu_2,2)$ dissociate within a few hundred femtoseconds after creation by a 403 nm pulse. We propose that the quantum beat is generated between states $(\nu_1,1,0)$ and $(\nu_1,0,0)$. In this case the beat is mainly between the states (6,1,0) and the (6,0,0), and to a lesser extent the (5,1,0) and (5,0,0) states. However, in the gas phase the separation between the (6,0,0) and the (5,0,0) state was found to be about 681 cm^{-1},[36] which is only slightly more than twice the bending mode frequency. This indicates also that a beat between the (6,0,0) and the (5,1,0) states is generated with almost the same frequency. The Fourier transform of the quantum beat typically has a FWHM of 15–20 cm^{-1}, and shows some asymmetry to higher frequencies. This makes it likely that two similar beat frequencies cause the quantum beat. Our time resolution, however, is insufficient to justify a detailed line shape analysis on the Fourier transform. With our time resolution and the spectral bandwidth of our laser pulses we are incapable of creating beats between the (5,1,0) and (6,1,0) states or the (6,0,0) and the (5,0,0) states.

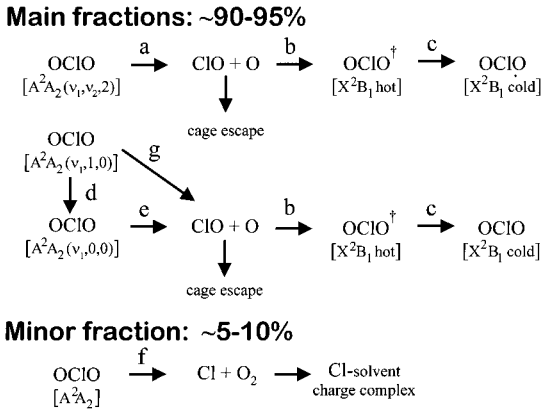

FIG. 8. Flow diagram representing dynamical pathways of OClO photochemistry in solution based on the results discussed in this paper.

Based on our data of the three solvents, we believe that the 1.3–1.5 ps decay is caused by relaxation from states $(\nu_1,1,0)$ to states $(\nu_1,0,0)$. For the various solvents this would include vibrational relaxation from (6,1,0) to (6,0,0) and from (5,1,0) to (5,0,0). A consequence of such relaxation is that we should observe an increase of stimulated emission accompanying this decay, the rise time of which should match the decay time of the quantum beat, which is exactly what we see in the 403 nm data of cyclohexane. The reason for this is that the gas phase absorption cross section for states $(\nu_1,0,0)$ is 1.6–2.1 times higher than for states $(\nu_1,1,0)$.[36] The observed increase in stimulated emission will, however, also depend on the relative intensity of the probe laser pulse at the respective frequencies for the relaxed and unrelaxed state. In combination with the different solvent shifts this explains the solvent dependence of the change in stimulated emission due to this relaxation process. Thus, we suggest that the lifetime of the single excited bending mode vibration on the $A\,^2A_2$ PES is 1.3–1.5 ps. Vibrational relaxation is known to occur on the picosecond time scale,[69] and the value found for the bending mode in the electronic excited $A\,^2A_2$ state can be compared to vibrational relaxation time scales of other small molecules like I_2,[7] I_2^-,[14,17–19] CN^-,[70,71] ClO^-,[72] and N_3^-.[73]

C. Flow scheme for the reaction pathways

As guidance to the discussion of our results we first present in Fig. 8 a flow scheme of the OClO photodissociation reaction based on our experimental results. As is clear from this scheme we describe the different processes as a series of consecutive first-order kinetic reaction steps:

$$A \xrightarrow{\tau_1} B \xrightarrow{\tau_2} C \xrightarrow{\tau_3} D. \quad (1)$$

Based on the scheme in Fig. 8 and information in Sec. III A, the signal at 267 nm is mainly fed by steps a and e, and decreases through step b for the ClO contribution; the feeding of a possible Cl–solvent charge transfer complex contribution at this wavelength is related to step f. The signal at 403 nm is influenced by the decay times τ of the steps a, c, d, e, and f, where steps a, c, e, and f lead to a reduction in probe transmittance, and step d can lead to both an increase and reduction in probe transmittance. The stimulated emission signal at 800 nm we assign to OClO molecules on the $A\,^2A_2$ PES, that do not immediately dissociate, and therefore can connect to steps d, e, and f. The positive contribution at 800 nm we ascribe to absorption of vibrationally hot $OClO^{\dagger}$ on the $X\,^2B_1$ surface to the $A\,^2A_2$ PES, that is related to steps b and c. Note, however, that the signal at 800 nm is observed halfway through the cascade of vibrational relaxation steps that brings the recombined hot $OClO^{\dagger}$ to the relaxed ground state. Therefore, the feeding time of step b is a lower limit for the feeding time of this signal, and the time for the ground state recovery should be slower than the ''decay time out'' (step c) at 800 nm.

The different fits we use to describe our experimental data are composed of signal contributions that decay exponentially after excitation

$$A(t)=\exp(-t/\tau_1), \tag{2}$$

contributions that are fed by one rate (τ_1) and decay by another (τ_2)

$$B(t)=\frac{\tau_2}{\tau_2-\tau_1}\cdot[\exp(-t/\tau_2)-\exp(-t/\tau_1)], \tag{3}$$

and contributions that are fed after two consecutive first-order reaction steps (τ_1,τ_2) and decay by a third (τ_3)

$$C(t)=\frac{\tau_3}{\tau_2-\tau_1}\cdot\left[\frac{\tau_2}{\tau_2-\tau_3}\cdot\exp(-t/\tau_2)-\frac{\tau_1}{\tau_1-\tau_3}\cdot\exp(-t/\tau_1)\right]-\left[\frac{\tau_2}{\tau_2-\tau_3}-\frac{\tau_1}{\tau_1-\tau_3}\right]\cdot\exp(-t/\tau_3). \tag{4}$$

These expressions are all normalized; that is, $A(t)+B(t)+C(t)+D(t)=1$ holds at all times (D is formed after the relaxation step with time constant τ_3). This implies that the relative weight they obtain in a fit function composed of a number of these expressions corresponds to the relative amount of molecules that have followed the corresponding pathway. The appropriate sum of contributions is convoluted with the Gaussian response function, and for the 267 and 800 nm probe data this Gaussian response function is also added at time-zero delay to account for the coherence (multiphoton absorption) contribution during time overlap. This contribution is not included in the fits of the 403/403 nm data, where a strong bleach before and a strong increased absorption after zero time delay clearly indicates that more complicated multiphoton processes contribute in the case of identical pump and probe pulse wavelengths.

The 403 nm pump pulse we used in our experiments creates about 45%–53% population in states (ν_1,0,0), about 32%–35% in states (ν_1,ν_2,2), and about 15%–20% in states (ν_1,1,0) (see Table I). The above flow scheme therefore suggests that in our experiments only one third of the excited molecules enters the direct dissociation channel associated with step a. In the next paragraphs we discuss the dynamics of OClO in solution for each solvent separately.

D. Cyclohexane

For OClO in cyclohexane no time-resolved measurements have been reported previously. However, Reid and co-workers have performed cw resonance Raman measurements on OClO in cyclohexane.[60,61]

1. Pump 400 nm—probe 267 nm

The signals with probing at 267 nm are shown in the upper panel of Fig. 5. In accordance with conclusions from previous work on OClO in water,[53–56,58,59] we assign these signals mainly to the ClO fragment (see Sec. III A). We note further that chlorine atoms in the gas phase do not absorb between 140 and 370 nm,[74] and we do not know if chlorine also forms a charge transfer complex with cyclohexane. The following equations provided excellent fits to the data.

Pump and probe polarization parallel:

$$S_{\parallel}(\tau)=\int_{-\infty}^{\infty}dt\{[0.57\cdot(1.02\cdot(e^{-t/8.9}-e^{-t/0.14}))+0.43\cdot(1-e^{-t/0.14})]\cdot H(t)\cdot A(t-\tau)\}+67\cdot A(\tau); \tag{5}$$

Pump and probe polarization perpendicular:

$$S_{\perp}(\tau)=\int_{-\infty}^{\infty}dt\{[0.49\cdot(1.02\cdot(e^{-t/8.9}-e^{-t/0.20}))+0.51\cdot(1-e^{-t/0.20})]\cdot H(t)\cdot A(t-\tau)\}+27\cdot A(\tau), \tag{6}$$

where $H(t)$ is the Heaviside function [$H(t\geqslant 0)=1$, and $H(t<0)=0$], and τ is the pulse delay time. The response is convoluted with the autocorrelation response function $A(\tau)$, which has a FWHM of 226 ± 15 fs for these measurements. The fit for both parallel and perpendicular probe polarization contains an exponential decay with 8.9 ps decay time and an offset, both with similar weights, to describe the decay rates of the ClO contribution. The only difference is the rise time that describes the formation of the ClO. We find a rise time of 140 fs for parallel and 200 fs for perpendicular probe polarization. The anisotropy decay function we constructed from these decays according to the formula

$$r(t)=\frac{S_{\parallel}(\tau)-S_{\perp}(\tau)}{S_{\parallel}(\tau)+2S_{\perp}(\tau)}, \tag{7}$$

shows a decay time of ~0.27 ps. These data suggest that ClO fragments are formed in cyclohexane with a 140 fs time constant (step a, Fig. 8), and that the ClO fragments obtain rotational momentum during the dissociation, which causes a depolarization decay with a 0.27 ps time constant. The 8.9 ps decay time we assign to recombination of ClO+O to OClO

(step b). Of the three solvents we studied, cyclohexane clearly has the slowest recombination time. If the remaining offset is only caused by ClO absorption the data suggest that for the formed ClO+O there is about a 43% chance that a fragment escapes from the solvent cage, when pumping at 400 nm. Note that we do not know if a possible chlorine–cyclohexane charge transfer complex contributes to the signal. More experiments are needed to clarify this issue.

From gas phase work it has been concluded that for excitation energies near 3.1 eV the dissociation process changes, which has been attributed to depositing sufficient energy into the OClO molecule for direct dissociation over a barrier.[42] This strongly suggests that full understanding of the OClO reaction dynamics involves knowledge over the entire four-dimensional space set up by the three vibrational coordinates and the potential energy. In other words: dissociation channels could depend on combinations of vibrational motions. The population is initially created on the $A\,^2A_2$ PES. In Sec. III B we proposed that the quantum beat is between states $(\nu_1,1,0)$ and $(\nu_1,0,0)$. Given PES cross sections calculated by Werner and Petersen[32] (Fig. 2), states that include excitation of the ν_3 coordinate are most likely to lead to rapid direct dissociation from the $A\,^2A_2$ state, and are therefore probably connected to the rise of the ClO absorption signal at 267 nm. This is also in agreement with conclusions from gas phase work, which indicate that the ClO yield is three times higher,[40] and the Cl yield ten times lower,[43] for modes with similar total excitation energy if the ν_3 mode is also excited.

2. Pump 403 nm—probe 403 nm

During the first picosecond OClO in cyclohexane shows a strong coherent artifact, followed by a decrease in bleaching up to ~300 fs, after which the bleach increases (see Figs. 4, 5). In contrast to water (*vide infra*), the bleach does not decay during the first 4 picoseconds and the signal reaches a minimum after about 4 ps. We also see a strong quantum beat superimposed on the signal with a beat period of 101 fs, which corresponds to an energy of 330 cm^{-1}. The amplitude of the quantum beat decreases with a decay time of 1.3 ps. The data are well described by the function (see Fig. 5, middle panel)

$$S(\tau)=\int_{-\infty}^{\infty} dt[-0.27\cdot(e^{-t/1.3})\cdot\cos(2\pi t/0.101) - 0.60\cdot e^{-t/0.1}-0.40-0.29\cdot(1-e^{-t/1.3})] \cdot H(t)\cdot A(t-\tau). \quad (8)$$

The width of the autocorrelation function was 55 fs. This fit consists of two parts. The first part is a two-component decay function that starts at time $t=0$, containing a decay time of 0.1 ps and an offset, with an oscillation superimposed on it with a time period of 101 fs and amplitude decay time of 1.3 ps. Due to the strong coherent artifact the ultrafast 0.1 ps decay time is not accurately determined. However, its existence is clear since the bleaching still drops between 200 and 300 fs, while the coherent artifact contribution after $t=0$ has an increased absorption signature. It seems logical to associate this 0.1 ps decay with the ClO formation (0.14 ps). Our calculations indicate that about 32% of the excited state population is in states $(\nu_1,\nu_2,2)$, which we expect to cause this component. The second part of the fit describes the increase of stimulated emission, with a 1.3 ps rise time, that becomes noticeable after 300 fs. This 1.3 ps rise time is considerably faster than the 8.9 ps decay time observed at 267 nm, and is therefore not related to recombination of ClO+O. The 1.3 ps rise time exactly matches the decay time of the quantum beat, strongly suggesting that the two are connected. In cyclohexane, which causes a 275 cm^{-1} redshift of the OClO absorption spectrum compared to the gas phase, the excited state superposition created by our pump pulse is dominated by the (6,0,0) and the (5,02) mode (see Fig. 3). To a lesser extent the (6,1,0), (5,1,0), and (4,1,2) modes contribute. Since we assume that states $(\nu_1,\nu_2,2)$ are associated with the nearly instantaneously formed ClO, the dynamics at 403 nm after a few hundred femtoseconds has to be related to states $(\nu_1,1,0)$ and $(\nu_1,0,0)$. The strongest contributions to this beat should come from the superposition of the (6,1,0) and the (6,0,0) mode, and the superposition of the (5,1,0) and the (6,0,0) mode. The relaxation from (6,1,0) to (6,0,0) results in the creation of a state with a 2.1 times higher oscillator strength,[36] and located close to the maximum of the laser pulse. Therefore, this relaxation should give rise to a strong increase of stimulated emission, which explains the rising of the bleach with the same time constant as the decay of the quantum beat. Since this rising contribution does not decay noticeably over the first 4 ps, the lifetime of the (6,0,0) state has to exceed 10 ps in cyclohexane. Consequently, a large part of the nondecaying offset signal is also related to stimulated emission from the (6,0,0) state.

3. Pump 400 nm—probe 800 nm

Probing at 800 nm we only observe a very strong coherence spike (Fig. 5, lower panel). In previous work on OClO in water and acetonitrile, signals were observed for this type of experiment.[53–56,58,59] For OClO in water, these signals were attributed to (increased) absorption from vibrationally hot OClO on the $X\,^2B_1$ surface to the $A\,^2A_2$ surface.[54–56,58,59] This vibrationally hot OClO was believed to be formed by recombination of ClO+O to OClO. The absence of a clear signal could be due to the longer recombination time. Obviously our data do not give evidence for this interpretation.

E. Acetonitrile

1. Pump 400 nm—probe 267 nm

Reid and co-workers have previously studied OClO reaction dynamics in acetonitrile, using subpicosecond pump probe spectroscopy[58,59] and time-resolved resonance Raman spectroscopy.[62] Their data showed a delayed rise, which they connected to a 2.2 ps decay time with negative amplitude, followed by a slow decay of ~15% of the signal during the first 20 ps, leaving a large offset.[58,59] Even though we notice the similarity between our signals at 267 nm (Fig. 6, upper panel) and those of Philpott *et al.*,[58,59] there are some significant differences in the dynamics we extract from it. This is mainly a result of our more than three times better time

resolution. In contrast to Philpott *et al.*[58,59] we find that the main rise of the signal shows no significant delay: after ~0.2 ps the signal has nearly reached maximum. Only an additional 7% increase appears to occur during the following 2.5 ps. This 7% signal rise is of comparable size to the slow noise oscillations between 18 and 24 ps delay; thus, it is not 100% certain that this is a real feature! Given that Phillpott *et al.*[58,59] observed a similar time delay (2.2 ps decay time) before reaching maximum, we are inclined to believe it is a real feature.

The data for both parallel and perpendicular pump and probe polarization show the same behavior. However, since the signal with perpendicular probe polarization has a lower signal/noise ratio, it cannot provide a critical test to the parameters obtained for parallel polarization. Therefore, we present only the fit data for parallel polarization (see Fig. 6).

Pump and probe polarization parallel:

$$S_{\parallel}(\tau)=\int_{-\infty}^{\infty} dt\{[0.22\cdot(1.54\cdot(e^{-t/6.0}-e^{-t/2.1}))+0.78] \cdot H(t)\cdot A(t-\tau)\}+38\cdot A(\tau), \tag{9}$$

where $A(\tau)$ has a FWHM of 240 fs. This fit suggests that 78% of the ClO fragments are formed almost instantaneously and do not recombine due to cage escape (the offset), formed immediately after excitation by the pump beam. Basically the rise time of this direct ClO formation is unresolvable with our time resolution, which indicates that it is in the range of 0–60 fs. The remaining 7% of the observed signal, which is related to ~22% of the dissociating molecules according to the fit function, is formed with a 2.1 ps time constant and disappears through recombination with a 6.0 ps time constant. Here, we point out that this fit is not unique. For instance the 2.1 ps/6.0 ps/22% combination can be replaced by 1.5 ps/7.0 ps/25%, a fit of comparable quality. Alternatively, part of the instantaneously formed ClO could also recombine, which we also found to give acceptable fits although requiring more fit parameters. A preference for which model to choose cannot be made with these data only. An appealing motivation for a lower recombination yield of the instantaneously formed fraction over the secondary fraction (found for both descriptions) is that ''impulsively'' formed ClO+O probably contains more translational kinetic energy, and therefore is more likely to escape the solvent cage. This argument is supported by the faster ClO formation time in acetonitrile compared to cyclohexane.

2. Pump 403 nm—probe 403 nm

The fit describing the 403 nm one-color pump probe signal in acetronitrile (Fig. 6) is

$$S(\tau)=\int_{-\infty}^{\infty} dt[-0.20\cdot(e^{-t/1.5})\cdot\cos(2\pi t/0.101) -0.34\cdot e^{-t/0.25}-0.66]\cdot H(t)\cdot A(t-\tau). \tag{10}$$

The FWHM of the function $A(t-\tau)$ is 55 fs. Philpott *et al.*[58,59] have shown that one third of the (offset) signal that does not noticeably decay during the first 6 ps eventually decays with a time constant of 37 ps. Note that the decay time for the quantum beat is similar to that observed for the data in cyclohexane.

Since there is no redshift of OClO in acetonitrile compared to the gas phase, our pulse mainly excites the (6,0,0) and (5,1,0) modes, and to a lesser extent the (4,1,2), (5,0,0), (4,0,2), (5,0,2), and the (6,1,0) modes. Due to the larger spectral broadening more states are significantly populated by the pump pulse in acetonitrile and water than in cyclohexane. Following our interpretation for cyclohexane, that the quantum beat decay is related to relaxation of the bending mode ν_2, seems to agree well with more excitation of the (5,1,0) than the (6,1,0) mode. The relaxed (5,0,0) state is located at a part of the probe pulse spectrum with a much lower intensity, which certainly compensates for the higher oscillator strength, and thereby could lead to no apparent increase of stimulated emission upon this relaxation. The offset should then be due to stimulated emission and bleach. The slow 37 ps decay obtained by Philpott *et al.*[58,59] at 400 nm could partially be due to restoration of the ground state absorption stemming from recombination of ClO+O to OClO. This decay process should be slower than the 6.0 ps recombination time found at 267 nm. Relaxation from the excited state to the ground state not involving dissociation could also contribute to this 37 ps decay.

In contrast to cyclohexane, in acetonitrile the initial fast 0.25 ps decay component is slower than the ClO formation time observed at 267 nm. At this point it is important to stress that the multiphoton coherence signal around zero delay time, which significantly distorts this signal during the first 200 fs, is not included in this fit. Therefore, care should be taken with the interpretation of this fast component.

3. Pump 400 nm—probe 800 nm

The function that describes the decay at 800 nm is (see Fig. 6, lower panel)

$$S(\tau)=\int_{-\infty}^{\infty} dt\{[-0.48\cdot e^{-t/1.5} +0.52\cdot(8.49\cdot e^{-t/7.2}+0.76\cdot e^{-t/2.1}-9.25\cdot e^{-t/6.0})] \cdot H(t)\cdot A(t-\tau)\}+6.7\cdot A(\tau). \tag{11}$$

The autocorrelation function $A(\tau)$ has a FWHM of 162 fs. Basically Eq. (11) consists of only two contributions. The first is a stimulated emission contribution that decays with a 1.5 ps decay time. The second contribution, a rising increased absorption, is related to the ClO+O formation and recombination. Apart from the weight of 0.52, the parameters of this contribution are based on the rise and decay time of the second fraction of ClO observed at 267 nm, and the 7.2 ps decay time has been determined by Philpott *et al.*[58] from a measurement that spans a 40 ps range. All other parameters of the second contribution are calculated from the expression for $C(t)$ in Eq. (4). Philpott *et al.*[58] previously assigned the negative stimulated emission signal contribution to a coherent artifact, which is highly unlikely given the long time it takes before the 800 nm negative signal changes into

an increased absorption signal. Given the agreement of the 1.5 ps decay time of this stimulated emission signal with the 1.5 ps decay time of the quantum beat, it is very tempting to connect both to the same vibrational motion on the $A\,^2A_2$ PES. Note that our time resolution in the 800 nm data is almost three times lower than for the 403 nm data; therefore, we can not resolve the quantum beat in the 800 nm data.

The increased absorption signal at 800 nm is assigned by Philpott *et al.*[58,59] to vibrational relaxation of ClOO, rather than OClO, to which similar signals in water are assigned.[54–56,58,59] Their main argument is that the increased absorption signal at 800 nm is somewhat stronger in acetonitrile (the peak is about 50% higher), while the cage escape clearly is higher, and therefore the recombination yield should be lower.[58,59] First, we remark that this argument depends on the conclusion that all OClO molecules initially dissociate, which clearly is in contradiction with our results. Second, a comparison of the apparent signal strength versus the actual amplitude in the fit function for our acetonitrile and water (*vide infra*) data at 800 nm, indicates that the same amount of recombined molecules give rise to about three times more increased absorption signal for acetonitrile. This is a consequence of two factors: (1) The very different ratio of the rise and decay time at 800 nm for the two solvents; (2) The increased absorption contribution in water peaks at an earlier delay time and the apparent peak height is therefore much stronger reduced by the stimulated emission contribution. Thus, assuming that the increased absorption signals in both water and acetonitrile are connected to the same species, our data indicate that in water twice as many molecules are responsible for the signal. Stated differently: the geminate recombination yield in water is two times higher than in acetonitrile. This demonstrates that it is not required to invoke the formation of ClOO in acetonitrile[58,59] versus OClO in water to explain a larger maximum signal strength at 800 nm in acetonitrile.

F. Water

1. Pump 400 nm—probe 267 nm

The reaction dynamics of OClO in solvents has been studied most intensively in water.[52–59,62–64] Data by the Keiding group[54,56] with probing in the range of 250 to 320 nm gave no indication of the formation of any significant fraction of ClOO in water. Recently, Thomsen *et al.*[57] demonstrated with time-resolved resonance Raman experiments that some ClOO is formed after excitation of ClOO in water. The ClOO formation process is 13 ps delayed and rises with a time constant of 28 ps. This indicates that ClOO does not influence the dynamics measured at 267 nm during the first 10 ps. In accordance with Keiding and co-workers[54–56] and the result of Thomsen *et al.*,[57] we assign the dynamics at 267 nm mainly to ClO.

The signal with probing at 267 nm (Fig. 7) shows a rapid decay with a time constant of about 2.5 ps, which levels off to about 20% of the maximum amplitude, after which no significant decay is observed up to 50 ps (cf. the data in Refs. 55, 56, 58). This residual offset signal has been assigned to the Cl–water charge transfer complex.[54] We obtain a better fit to our data with two decay exponents, 1.2 and 4.1 ps, and an offset. This biexponential decay we ascribe to recombination of ClO+O to form vibrationally hot OClO on the ground state PES. Signals for both parallel and perpendicular polarization have been measured, that can be described using the same decay parameters, with only small modifications in the weights of the different components (see Fig. 7, upper panel). The fit functions that describe our data are:

Pump and probe polarization parallel:

$$\begin{aligned} S_{\parallel}(\tau) = \int_{-\infty}^{\infty} dt \{ & [0.32 \cdot (1.02 \cdot (e^{-t/4.1} - e^{-t/0.08})) \\ & + 0.51 \cdot (1.07 \cdot (e^{-t/1.2} - e^{-t/0.08})) \\ & + 0.17 \cdot (1 - e^{-t/0.08})] \\ & \cdot H(t) \cdot A(t-\tau) \} + 26 \cdot A(\tau), \end{aligned} \tag{12}$$

Pump and probe polarization perpendicular:

$$\begin{aligned} S_{\perp}(\tau) = \int_{-\infty}^{\infty} dt \{ & [0.41 \cdot (1.03 \cdot (e^{-t/4.1} - e^{-t/0.13})) \\ & + 0.39 \cdot (1.12 \cdot (e^{-t/1.2} - e^{-t/0.13})) \\ & + 0.20 \cdot (1 - e^{-t/0.13})] \\ & \cdot H(t) \cdot A(t-\tau) \} + 13 \cdot A(\tau). \end{aligned} \tag{13}$$

The FWHM of the autocorrelation $A(\tau)$ is 245 fs. A significant difference is found in the rise time of the two signals: 80 fs for parallel pump and probe polarization and 130 fs for perpendicular polarization. Similar to the difference we observed in cyclohexane, we again ascribe it to the ClO fragment picking up rotational momentum during the bond-breaking process. We extract a 0.17 ps anisotropy decay time for the ClO fragment in water, and a 80 fs ClO formation time.

2. Pump 403 nm—probe 403 nm

The signal at 403 nm shows a strong coherent artifact followed by a bleaching that decreases for 0.7 ps, and then increases again up to about 1.5 ps, whereafter it decays with an average time constant of 4 ps (Fig. 7, middle panel). The initial drop followed by an increase has not previously been identified by others.[53–56,58,59] It has been shown that at longer delay times the signal levels off to a tiny residual offset related to the yield of the $Cl+O_2$ channel, which has been estimated at 7%–10%.[53–55,58] Superimposed on the decay we observe a quantum beat, with an amplitude decay time of 1.5 ps, and a beat frequency corresponding to 330 cm^{-1} (101 fs), an identical frequency and comparable decay time as that observed in cyclohexane and acetonitrile.

Due to the rise and decay on comparable time scales, the fit of these data becomes quite complicated. An example of an equation that describes the data fairly well is (compare Fig. 7)

$$S(\tau)=\int_{-\infty}^{\infty} dt[-0.28\cdot(e^{-t/1.5})\cdot\cos(2\pi t/0.101) - 0.57\cdot e^{-t/0.3}-0.43\cdot e^{-t/5.1} - 1.27\cdot(4.0\cdot(e^{-t.2.0}-e^{-t/1.5}))] \cdot H(t)\cdot A(t-\tau). \quad (14)$$

In our opinion, fitting these data requires too many similar decay times. Therefore, we do not wish to attach too much significance to most numbers in this fit. The main exception is the 1.5 ps quantum beat decay time, since the beat can be separated from the total dynamics. This decay we again assign to vibrational relaxation from states $(\nu_1,1,0)$ to states $(\nu_1,0,0)$, which also accounts for the increase of stimulated emission after 0.7 ps. The dynamics described by the fit consists of: (1) dissociation from $(\nu_1,\nu_2,2)$ states (0.3 ps component); (2) a 5.1 ps ground state absorption recovery time (obtained by Philpott *et al.*[58,59] from fitting over a 60 ps range); (3) a 1.5 ps decay time of $(\nu_1,1,0)$ states (responsible for quantum beat decay and a rising stimulated emission). The 2.0 ps decay time of states $(\nu_1,0,0)$ populated by relaxation from $(\nu_1,1,0)$ should not be taken too literally. However, a $(\nu_1,1,0)$ to $(\nu_1,0,0)$ relaxation faster than 2 ps could not cause a second minimum at ~1.5 ps, and a decay of $(\nu_1,0,0)$ states slower than ~4 ps is inconsistent with a 5.1 ps ground state recovery. A single exponential fit between 2 and 6 ps time delay gives a 3.8 ps decay time, indicating a faster than 5.1 ps decay during the first 6 ps. Therefore, it is justified to conclude that from the $(\nu_1,0,0)$ state OClO either dissociates followed by recombination or directly relaxes to the OClO ground state with a 2–4 ps decay rate. The dissociation option is appealing since it also could explain the biexponentiality of the 267 nm decay.

Thøgersen *et al.*[55] found a ground state recovery time of 10 ps using 390 nm for both pump and probe. This suggests that the actual numbers are very sensitive to the excitation wavelength. Here, the signal does not reach maximum before 2 ps. This rising behavior is not addressed by them;[55] however, this feature might be a reason for their conclusion of instantaneous dissociation followed by recombination within 0.8 ps.

3. Pump 400 nm—probe 800 nm

The data at 800 nm are shown in the lower panel of Fig. 7. We have fitted the data using a stimulated emission contribution, that decays with 1.5 ps, and an increased absorption contribution. As with acetonitrile, only the weight factor is a fit parameter for the increased absorption contribution. Unlike for the acetonitrile data, the fit quality is far from perfect. An explanation for this is that the 267 nm data describe the recombination time of ClO+O to OClO, which is not the same as the appearance time in the ground state vibrational levels where absorption to the excited state can occur with 800 nm light. A perfect fit of the changeover from stimulated emission to increased absorption is obtained if the increased absorption contribution is delayed by 0.55 ps. Given the above argument, such a delay could be justified. For acetonitrile the introduction of such a delay was probably not required since the recombination time was found to be 6.0 ps, five times longer than the main recombination time in water. The decay of the increased absorption is also perfectly described if we only use the contribution from the 1.2 ps decay at 267 nm instead. Even though we do not see a justification for omitting the 4.1 ps related fraction, we present here the equation that gives a perfect fit to the data (see Fig. 7)

$$S(\tau)=\int_{-\infty}^{\infty} dt\{[-0.25\cdot e^{-t/1.5}\cdot H(t)+0.75 \cdot(0.08\cdot e^{-(t-0.55)/0.08}+1.50\cdot e^{-(t-0.55)/1.2} - 1.58\cdot e^{-(t-0.55)/0.7})\cdot H(t-0.55)] \cdot A(t-\tau)\}+10\cdot A(\tau). \quad (15)$$

As for acetonitrile we propose that the stimulated emission originates from population on the OClO $A\,^2A_2$ excited state PES. This signal is very likely connected to the population fraction that is responsible for the quantum beat in the 403 nm/403 nm data, that also decays with a 1.5 ps time constant. With regard to the second contribution, we follow the interpretation by Keiding and co-workers[54,56] that this absorption is related to a transient vibrationally hot species on the $X\,^2B_1$ surface, that apparently transits the 800 nm window with an average decay time of 0.7 ps [see Eq. (15)].

TABLE I. Parameters concerning the initial degree of excitation of the different vibronic states.

Solvent	Initial population in states $(\nu_1,0,0)$	$(\nu_1,1,0)$	$(\nu_1,\nu_2,2)$
Cyclohexane	53%	15%	32%
Acetonitrile	45%	20%	35%
Water	45%	20%	35%

G. Comparison for the different solvents and conclusions

In Tables I, II, and III we summarize some of the parameters that we extracted from the data analysis in Secs. III D–III F. The error margins on the wavelength of the laser pulse and the redshift of the absorption spectra can only noticeably influence the relative population of the three fractions indicated in Table I for the cyclohexane data. This is a conse-

TABLE II. Parameters concerning the recombination yield of those molecules that dissociated to ClO+O.

Solvent	Fraction of recombination of initially dissociated molecules: Total	1st fraction	2nd fraction	Fraction of cage escape
Cyclohexane	⩾57%	57%	⋯	43%
Acetonitrile	⩾22%	0%	22%	78%
Water	⩾83%	51%	32%	17%

TABLE III. Values for the decay parameters in the different solvents, corresponding to the dynamical steps a–e presented in Fig. 5. The time constant τ_g denotes a secondary dissociation process mentioned in the text. The ground state recovery time is indicated by τ_{recover}.

Solvent	τ_a	τ_b	τ_c ($\lambda = 800$ nm)	τ_d ($=\tau_{QB}$)	τ_e	τ_g	τ_{recover}
Cyclohexane	140 ± 30 fs	8.9 ± 0.9 ps	?	1.3 ± 0.15 ps	?(>10 ps)		?
Acetonitrile	0 fs ($\leqslant$60 fs)	6.0 ± 1.5 ps	7.2 ps (Ref. 58)	1.5 ± 0.2 ps	?(>10 ps)	2.1 ± 0.6 ps	36.9 ps (Ref. 58)
Water	80 ± 15 fs	a) 1.2 ± 0.2 ps b) 4.1 ± 0.5 ps	0.7 ± 0.3 ps ($\leqslant$1.4 ps)	1.5 ± 0.2 ps	''2.0 ps'' (2–4 ps)		5.1 ps (Ref. 58)

quence of the much smaller spectral broadening of the cyclohexane absorption spectrum by solvent–solute interactions.

The observation of a quantum beat in the 403 nm data for all solvents proves beyond any doubt that not all OClO molecules dissociate within the first picosecond after excitation. The 1.3–1.5 ps decay we ascribe to the relaxation from $(\nu_1,1,0)\rightarrow(\nu_1,0,0)$. This relaxation process explains at the same time the rise of the stimulated emission in cyclohexane and water, that for cyclohexane can be shown to occur with the same time constant as the decay of the quantum beat. For water the fit is too complicated to allow us to draw such a strong conclusion.

The 267 nm data demonstrate that a fraction of the molecules dissociates very fast. We ascribe the almost instantaneously rising signal to molecules dissociating from states $(\nu_1,\nu_2,2)$. This implies that in all cases about one third of the excited state molecules (see Table I) dissociates within a few hundred femtoseconds. In this respect our interpretation deviates from the conclusions drawn in previous studies of OClO photodissociation in solution, where all molecules are supposed to dissociate within much less than 1 picosecond.[53–56,58,59] In Table III we show that this direct dissociation step occurs with a time constant (τ_a) of 140, 80, and $\leqslant$ 60 fs, for cyclohexane, water, and acetonitrile, respectively. In the case of cyclohexane and water an anisotropy decay time of the polarization was extracted of 0.27 and 0.17 ps, respectively. This confirms that at 267 nm we deal with an increased absorption contribution of a reaction product, ClO, that acquires rotational momentum during formation.

In acetonitrile we identify a second slower dissociation fraction, with a 2.1 ps (τ_g in Table III) formation time. Assuming that the 78% of dissociated OClO [fast fraction; see Eq. (9)] that does not recombine in acetonitrile is related to the 35% population in states $(\nu_1,\nu_2,2)$ (see Table I), then this second slower fraction corresponds to 10% of the original excited state population. This fraction is either formed in competition with the relaxation from $(\nu_1,1,0)\rightarrow(\nu_1,0,0)$, or by dissociation from the dark $1\,^2B_2$ or $1\,^2A_1$ states. These numbers suggest that in acetonitrile 55% $(100-35-10)$ of the molecules do not dissociate at all. We have not found evidence for a secondary dissociation process in cyclohexane. Therefore, if only $(\nu_1,\nu_2,2)$ states dissociate in cyclohexane, 68% of the OClO molecules should not dissociate. In water a second channel probably also exists in view of the clearly biexponential recombination decay (step b) found in the 267 nm data. If the fraction with the 1.2 ps recombination time [51% in Eq. (12)] and the offset [17% in Eq. (12)] are related to ClO formed from the $(\nu_1,\nu_2,2)$ states (i.e., 68% of the 267 nm signal corresponds to 35% of the initial population; see Table I), than the fraction with the 4.1 ps recombination time [32% in Eq. (12)] should correspond to about 16% $(35\cdot32/68)$ of the initial excited state population. Combining these numbers indicates that in water 49% $(100-35-16)$ of the molecules have not dissociated.

For the 800 nm signal we argue that twice as many molecules contribute to the increased absorption contribution of the 800 nm signal in water than in acetonitrile, even though this signal appears to be stronger in acetonitrile. Based on the numbers above, in water 42% of the initially excited molecules dissociate and recombine (26% from the 1.2 ps recombination, and 16% from the 4.1 ps recombination). In acetonitrile this number is only 10%, so there is a discrepancy of a factor of 2! This line of argumentation does not include contributions from radiationless relaxation through the dark states to the ground state. The data of Phillpott *et al.*[58,59] on the ground state absorption recovery at 400 nm show a residual offset (after 150 ps) of about 11% of the amplitude at time zero for water and 67% for acetonitrile. Depending on whether one assumes that the 67% offset consists of only bleach or both bleach and stimulated emission, this offset implies that after 150 ps 33% or 50% of the molecules have recovered to the ground state in acetonitrile. For water, estimates of the ground state recovery are in the range of 80%–90%. These numbers indicate that 2–3 times more OClO molecules recover in water than in acetonitrile, in accordance with the previously mentioned factor of 2. The increased absorption at 800 nm in both water and acetonitrile is well described using decay time parameters extracted from the 267 nm data.

A second proof that not all OClO molecules dissociate within the first picosecond was found in the 800 nm data for water and acetonitrile. In both solvents these data clearly contain a stimulated emission contribution that decays with 1.5 ps. This signal we assigned to the same optical transition that leads to the increased absorption at 800 nm.

In conclusion: We have found clear indications that the fate of the excited electronic state of OClO in solution depends on which vibronic state is created. All in all, the reaction dynamics scheme of OClO in solution that emerges from our data is far more complex than presented so far.

ACKNOWLEDGMENTS

H.F. gratefully acknowledges financial support by the Swedish Natural Science Research Council. This work has benefitted from financial support through the EU-TMR Program (Contract Number MBI-97-005-01).

[1] V. Vaida and J. D. Simon, Science **268**, 1443 (1995).
[2] V. Vaida, S. Solomon, E. C. Richard, E. Ruhl, and A. Jefferson, Nature (London) **342**, 405 (1989).
[3] M. J. Rosker, M. Dantus, and A. H. Zewail, Science **241**, 1200 (1988).
[4] M. J. Rosker, T. S. Rose, and A. H. Zewail, Chem. Phys. Lett. **146**, 175 (1988).
[5] R. M. Bowman, M. Dantus, and A. H. Zewail, Chem. Phys. Lett. **161**, 297 (1989).
[6] M. Dantus, R. M. Bowman, and A. H. Zewail, Nature (London) **343**, 737 (1990).
[7] A. L. Harris, J. K. Brown, and C. B. Harris, Annu. Rev. Phys. Chem. **39**, 341 (1988).
[8] R. Zadoyan, Z. Li, C. C. Martens, and V. A. Apkarian, J. Chem. Phys. **101**, 6648 (1994).
[9] C. Lienau and A. H. Zewail, J. Phys. Chem. **100**, 18629 (1996).
[10] C. J. Bardeen, J. Che, K. R. Wilson, V. V. Yakovlev, V. A. Apkarian, C. C. Martens, R. Zadoyan, B. Kohler, and M. Messina, J. Chem. Phys. **106**, 8486 (1997).
[11] M. J. J. Vrakking, D. M. Villeneuve, and A. Stolow, J. Chem. Phys. **110**, 2474 (1996).
[12] L. Poth, Q. Zhong, J. V. Ford, and A. W. Castleman, Jr., J. Chem. Phys. **109**, 4791 (1998).
[13] J. M. Papanikolas, V. Vorsa, M. E. Nadal, P. J. Campagnola, J. R. Gord, and W. C. Lineberger, J. Chem. Phys. **97**, 7002 (1992).
[14] P. K. Walhout, J. C. Alfano, K. A. M. Thakur, and P. F. Barbara, J. Phys. Chem. **99**, 7568 (1995).
[15] E. Gershgoren, E. Gordon, and S. Ruhman, J. Chem. Phys. **106**, 4806 (1997).
[16] U. Banin, A. Waldman, and S. Ruhman, J. Chem. Phys. **96**, 2416 (1992).
[17] U. Banin and S. Ruhman, J. Chem. Phys. **98**, 4391 (1993).
[18] G. Ashkenazi, U. Banin, A. Bartana, R. Kosloff, and S. Ruhman, Adv. Chem. Phys. **100**, 229 (1997).
[19] T. Kühne, R. Küster, and P. Vöhringer, J. Chem. Phys. **105**, 10788 (1996).
[20] T. Kühne, R. Küster, and P. Vöhringer, J. Phys. Chem. A **102**, 4177 (1998).
[21] R. M. Bowman, M. Dantus, and A. H. Zewail, Chem. Phys. Lett. **156**, 131 (1989).
[22] N. Pugliano, D. K. Palit, A. Z. Szarka, and R. M. Hochstrasser, J. Chem. Phys. **99**, 7273 (1993).
[23] U. Marvet, Q. Zhang, E. J. Brown, and M. Dantus, J. Chem. Phys. **109**, 4415 (1998).
[24] Q. Zhang, U. Marvet, and M. Dantus, J. Chem. Phys. **109**, 4428 (1998).
[25] A. Arkell and I. Schwager, J. Am. Chem. Soc. **89**, 5999 (1967).
[26] K. Johnsson, A. Engdahl, P. Ouis, and B. Nelander, J. Phys. Chem. **96**, 5778 (1992).
[27] H. S. P. Müller and H. Willner, J. Phys. Chem. **97**, 10589 (1993).
[28] L.-H. Lai, C.-P. Liu, and Y.-P. Lee, J. Chem. Phys. **109**, 988 (1998).
[29] C. J. Pursell, J. Conyers, P. Alapat, and R. Parveen, J. Phys. Chem. **99**, 10433 (1995).
[30] C. J. Pursell, J. Conyers, and C. Denison, J. Phys. Chem. **100**, 15450 (1996).
[31] C.-P. Liu, L.-H. Lai, Y.-Y. Lee, S.-C. Hung, and Y.-P. Lee, J. Chem. Phys. **109**, 978 (1998).
[32] K. A. Peterson and H.-J. Werner, J. Chem. Phys. **96**, 8948 (1992).
[33] K. A. Peterson and H.-J. Werner, J. Chem. Phys. **105**, 9823 (1996).
[34] K. A. Peterson, J. Chem. Phys. **109**, 8864 (1998).
[35] E. C. Richard and V. Vaida, J. Chem. Phys. **94**, 153 (1991).
[36] S. Hubinger and J. B. Nee, Chem. Phys. **181**, 247 (1994).
[37] S. Michielsen, A. J. Merer, S. A. Rice, F. A. Novak, K. F. Freed, and Y. Hamada, J. Chem. Phys. **74**, 3089 (1981).
[38] P. A. McDonald and K. K. Innes, Chem. Phys. Lett. **59**, 562 (1978).
[39] E. C. Richard and V. Vaida, J. Chem. Phys. **94**, 163 (1991).
[40] E. Bishenden and D. J. Donaldson, J. Chem. Phys. **99**, 3129 (1993).
[41] E. Bishenden and D. J. Donaldson, J. Chem. Phys. **101**, 9565 (1994).
[42] H. F. Davis and Y. T. Lee, J. Chem. Phys. **105**, 8142 (1996).
[43] H. F. Davis and Y. T. Lee, J. Phys. Chem. **96**, 5681 (1992).
[44] R. F. Delmdahl, S. Baumgärtel, and K.-H. Gericke, J. Chem. Phys. **104**, 2883 (1996).
[45] M. Roth, C. Maul, and K.-H. Gericke, J. Chem. Phys. **107**, 10582 (1997).
[46] A. Furlan, H. A. Scheld, and J. R. Huber, J. Chem. Phys. **106**, 6538 (1997).
[47] C. J. Kreher, R. T. Carter, and J. R. Huber, Chem. Phys. Lett. **286**, 389 (1998).
[48] T. Baumert, J. L. Herek, and A. H. Zewail, J. Chem. Phys. **99**, 4430 (1993).
[49] P. Ludowise, M. Blackwell, and Y. Chen, Chem. Phys. Lett. **273**, 211 (1997).
[50] R. C. Dunn, E. C. Richard, V. Vaida, and J. D. Simon, J. Phys. Chem. **95**, 6060 (1991).
[51] R. C. Dunn and J. D. Simon, J. Am. Chem. Soc. **114**, 4856 (1992).
[52] R. C. Dunn, B. N. Flanders, and J. D. Simon, J. Phys. Chem. **99**, 7360 (1995).
[53] Y. J. Chang and J. D. Simon, J. Phys. Chem. **100**, 6406 (1996).
[54] J. Thøgersen, C. L. Thomsen, J. Aa. Poulsen, and S. R. Keiding, J. Phys. Chem. A **102**, 4186 (1998).
[55] J. Thøgersen, P. U. Jepsen, C. L. Thomsen, J. Aa. Poulsen, J. R. Byberg, and S. R. Keiding, J. Phys. Chem. A **101**, 3317 (1997).
[56] J. A. Poulsen, C. L. Thomsen, S. R. Keiding, and J. Thøgersen, J. Chem. Phys. **108**, 8461 (1998).
[57] C. L. Thomsen, M. P. Philpott, S. C. Hayes, and P. J. Reid, J. Chem. Phys. **112**, 505 (2000).
[58] M. J. Philpott, S. Charalambous, and P. J. Reid, Chem. Phys. Lett. **281**, 1 (1997).
[59] M. J. Philpott, S. C. Hayes, and P. J. Reid, Chem. Phys. **236**, 207 (1998).
[60] A. P. Esposito, C. E. Foster, R. A. Beckman, and P. J. Reid, J. Phys. Chem. A **101**, 5309 (1997).
[61] P. J. Reid, A. P. Esposito, C. E. Foster, and R. A. Beckman, J. Chem. Phys. **107**, 8262 (1997).
[62] S. C. Hayes, M. P. Philpott, S. G. Mayer, and P. J. Reid, J. Phys. Chem. A **103**, 5534 (1999).
[63] C. E. Foster and P. J. Reid, J. Phys. Chem. A **102**, 3514 (1998).
[64] S. C. Hayes, M. J. Philpott, and P. J. Reid, J. Chem. Phys. **109**, 2596 (1998).
[65] O. Dühr, E. T. J. Nibbering, and G. Korn, Appl. Phys. B: Lasers Opt. **67**, 525 (1998).
[66] F. Tschirschwitz and E. T. J. Nibbering, Chem. Phys. Lett. **312**, 169 (1999).
[67] W. Bray, Z. Phys. Chem., Stoechiom. Verwandtschaftsl. **54**, 569 (1906).
[68] U. K. Kläning and T. Wolff, Ber. Bunsenges. Phys. Chem. **89**, 243 (1985).
[69] J. C. Owrutsky, D. Raftery, and R. M. Hochstrasser, Annu. Rev. Phys. Chem. **45**, 519 (1994).
[70] E. J. Heilweil, F. E. Doany, R. Moore, and R. M. Hochstrasser, J. Chem. Phys. **76**, 5632 (1982).
[71] P. Hamm, M. Lim, and R. M. Hochstrasser, J. Chem. Phys. **107**, 10523 (1997).
[72] M. Lim, S. Gnanakaran, and R. M. Hochstrasser, J. Chem. Phys. **106**, 3485 (1997).
[73] P. Hamm, M. Lim, and R. M. Hochstrasser, Phys. Rev. Lett. **81**, 5326 (1998).
[74] *CRC Handbook of Chemistry and Physics*, 63rd edition (CRC, Boca Raton, 1982).